ORGANIC & BIOMOLECULAR CHEMISTRY

ARTICLE

The preference for dual-gold(I) catalysis in the hydro(alkoxylation vs phenoxylation) of alkynes

Received 00th January 20xx,
Accepted 00th January 20xx

DOI: 10.1039/x0xx00000x

www.rsc.org/

Èric Casals-Cruañas,[a] Oscar F. González-Belman,[a] Pau Besalú-Sala,[a] David J. Nelson,[b] and Albert Poater[a]*

Dinuclear gold complexes and their use in catalysis have received significant recent attention, but there are few critical comparisons of mono- *versus* dual gold-catalysed pathways. Herein we study the hydroalkoxylation and hydrophenoxylation of alkynes using density functional theory calculations, and compare two possible mechanisms that have been proposed previously on the basis of theoretical and experimental studies, which unravel different preferences because of both the nature of the alkyne and alcohol, as well as the non-innocent role of the counter-anion of the dual gold based catalyst. Entropy is found to have a significant effect, rendering the nucleophilic attack of the monoaurated intermediate [Au(L)(η^2-alkyne)]$^+$ difficult both kinetically and thermodynamically; this mechanism cannot easily form only the *trans*-alkene product that is observed experimentally. Instead, reaction *via* a dual gold catalysed mechanism presents much lower barriers. In addition, for the sake of direct comparison with recent results by Belanzoni, Zuccaccia, oversimplification of the *N*-heterocyclic carbene (NHC) ligand in the calculations might decrease the enthalpy barrier and lead to results that are not directly applicable to experiment. Moreover, the alkylic or arylic nature of the alkyne and/or alcohol is also tested.

Introduction

Due to recent and rapid advances in organogold chemistry and gold catalysis,[1-3] entire suites of gold catalysts and gold-catalysed reactions are now at the disposal of synthetic chemists.[4-10] While most of these transformations are enabled by well-defined [Au(X)(L)] complexes (where L is typically a phosphine or *N*-heterocyclic carbene (NHC) ligand), it was assumed that the transformations catalysed by gold could be summarised by the simple activation of the substrate by one molecule of gold catalyst. However, more recently the importance of *dual* gold catalysis, by means of cycloisomerization reactions first proposed by Toste and Houk,[11] and Gagosz,[12] and later established for many synthetic protocols.[13, 14] Well-defined digold pre-catalysts are now used for a number of applications.[15-23]

Dual gold catalysis might help to overcome the hurdle that Au^I has only two coordination sites available, with a linear geometry.[24] Another issue that remains is that understanding how ligand structure affects reactivity in catalysis, although some useful empirical observations have been made.[25] The coordination of phosphines to the gold centre stabilise it and allows for improved reactivity.[26] NHC ligands provide an alternative steric profile,[27] and allow for different levels of σ-donation and π-backbonding,[28-33] which modifies the interactions of the gold complex with substrates that are bound *trans*- to the NHC. The highest catalytic turnover numbers (TONs) were obtained by Hashmi and coworkers.[34, 35]

In the most common reactivity manifold, a gold-alkyne (or –alkene or –allene) complex is activated towards nucleophilic attack by a reagent such as an amine or an alcohol.[36] The counterion has been found to be non-innocent,[37] especially if it has the capacity to coordinate gold directly,[38-45] with the potential power to modify not only the catalytic activity but the regioselectivity and stereoselectivity of the reaction.

However, the potential activity of a second molecule of gold catalyst cannot be neglected; Toste and Houk have described two types of digold species: σ,π-digold acetylides and *gem*-diaurated complexes. This has stimulated a search for catalysts and reactions that specifically involve two gold centres.

Roithová and co-workers reported a digold mechanism for the methoxylation of alkynes.[46, 47] However, there is much ongoing debate about the relative competence of mono- and digold mechanisms for many gold-catalysed reactions. Even in situations where dual metal-catalysed mechanisms were not thought to be operative, there are some recent examples where calculations revealed cooperative effects; for example, there are examples of heterogeneous catalysis where changing the surface allowed adjacent sites to achieve cooperative catalysis.[48, 49]

The Nolan group has reported dual gold catalysed reactions in which reactivity is achieved not through the activation of a substrate with two molecules of gold catalyst, but via the interaction of two activated substrate molecules. Intermolecular hydrophenoxylation, hydroalkoxylation, and

[a] *Institut de Química Computacional i Catàlisi, Departament de Química, University de Girona, Campus de Montilivi sn, 17003 Girona, Catalonia, Spain.*
[b] *WestCHEM Department of Pure and Applied Chemistry, University of Strathclyde, Thomas Graham Building, 295 Cathedral Street, Glasgow, G1 1XL, UK.*

Electronic Supplementary Information (ESI) available: Frontier molecular orbital analysis and conceptual DFT, data for H- and F-substituted alkynes. Free Energy profiles for [{Au(IPr)}$_2$(μ-OH)]$^+$. See DOI: 10.1039/x0xx00000x

hydrocarboxylation reactions have been enabled by the use of well-defined [{Au(NHC)}$_2$(μ-OH)][X] complexes.[16-18] [{Au(NHC)}$_2$(μ-OH)][BF_4][50] combines the role of a Brønsted base [Au(OH)(NHC)][51] and a Lewis acid [Au(NHC)][BF_4]. These form [Au(NHC)(η2-alkyne)][36] and [Au(NHC)(OR)][52, 53] *in situ*, which react together to deliver the product (Scheme 1). Interestingly, the same research group found out that water is fundamental for such a reaction, except for studies with phenols and aryl alkynes.[11,56] Further, Nolan and Reek have recently confirmed the need for dual gold catalysis by encapsulation of the hydroxylated gold dimer.[54]

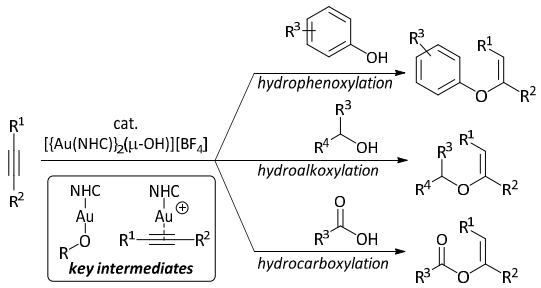

Scheme 1. Hydrophenoxylation, hydroalkoxylation, and hydrocarboxylation of alkynes catalysed by a digold complex.

The hydrophenoxylation protocol allows much milder reaction conditions to be used, together with lower loadings of gold, when compared to protocols that rely on monogold catalysts.[55, 56] However, in 2016 Zuccaccia and co-workers described the mechanism for the hydroxylation of alkynes,[37] accurately predicting the enthalpy barriers due to past benchmarking studies of the hydroamination of alkynes by Belpassi, Belanzoni and coworkers.[57]

It is possible for hydroalkoxylation to follow a mono- or dual-gold based mechanism.[58-60] Ujaque et al have previously studied the monogold catalysed hydrophenoxylation reaction, noting interactions with the counterion at various stages.[61] However, the hydrophenoxylation of diphenylacetylene with phenol (monitored by GC-FID) confirmed that the reactivity of [{Au(IPr)}$_2$(μ-OH)][X] decreased in the following order for X: SbF_6= BF_4 = FABA > OTf > NTf_2, which is in direct contrast with recent reports on the effect of the counter ion on the gold-catalysed hydroalkoxylation of alkyl alkynes.[28] In the latter reports the counter ion plays a crucial role in stabilizing key intermediates and aiding the protodeauration step, in which the counter ion acts as a proton shuttle. In contrast, the interaction of alkynes and alcohols of aliphatic character follow a monometal mechanism, bearing the nature of the rate determining state.[35,36] but again this preference is really weak since the use of phosphines instead of NHCs can lead to a dual gold mechanism.[35,37,38] For the latter results both gold moieties do not cooperate separately, *i.e.,* each one bonded to either the alcohol or the alkyne, but both are bound to the alkyne. The combination that involves an aryl alkyne with alcohols leads to uncertain results about the nature of the corresponding mechanism.[12]

Here, a thorough investigation of the mechanistic aspects of the mono- and dual gold-catalysed hydroalkoxylation of alkynes is conducted using computational methods, in order to probe the new reactivity exhibited in this transformation by recent experiments and calculations, where the assistance by a second alcohol molecule is said to be fundamental for the hydroalkoxylation of alkynes that lead to *trans*-alkenes.[28] Tools such as steric maps allow the characterisation of the steric environment of the catalysts and intermediates, giving further insight into their structure and properties. This detailed mechanistic study contributes to the expansion of our knowledge of this type of functionalisation of alkynes by gold catalysis.

Results and Discussion

Both mechanisms (mono- and dual-gold catalysed) were studied with the M06/TZVP~sdd//BP86/SVP~sdd DFT recipe described in the Computational Details (*vide infra*) for the sake of consistency, taking into account the significant demand on computational resources involved in considering intermediates and transition states on the dual gold-catalysed pathway that contain two 5d metals. Chloroform was used as the reference solvent for this study because it was used in the experimental study of Zuccaccia and coworkers,[37] maintaining the pressure at 1 atm for the sake of a direct comparison, even though all structures were calculated at 1354 atm[62-64] in our previous work;[65] the SI includes the values calculated at 1354 atm, which display no significant differences.

Monogold Catalysis

The monogold mechanism requires the reaction of η^2-alkyne complex **I** with an alcohol (Scheme 2). This mechanism requires nucleophilic attack by either one or two alcohol molecules. Intermediates include the adduct between species **I** and the incoming alcohol (**A**) and the alkoxylated intermediate **P** which exists prior to loss of H^+ and protodeauration. However this step is not discussed in detail here because experiments by Zuccaccia and co-workers suggest that it is not as important as the C-O bond forming step (i.e. the nucleophilic attack is rate determining).[37] In their recent study the methodology B2PLYP/def2-TZVP~sdd//BP86/def2-TZVP~sdd was used,[66-68]

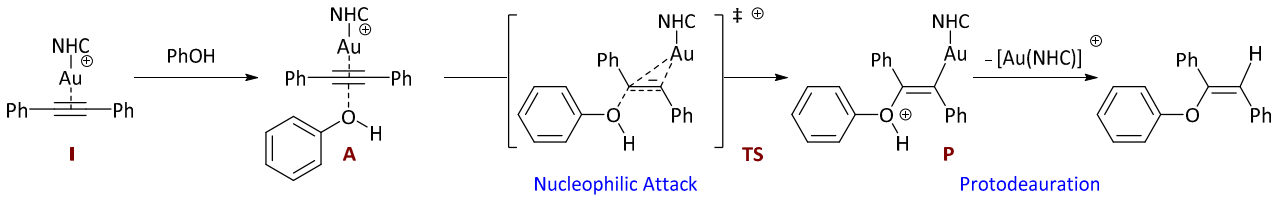

Scheme 2. Mechanism of the mono-gold catalysed hydrophenoxylation of alkynes.

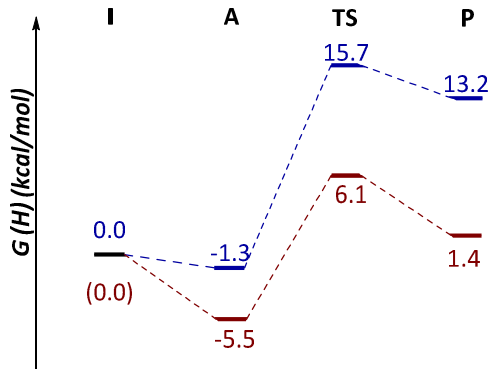

Figure 1. Free energy (**blue**) *versus* enthalpy (**red**) in the reaction of methanol with [Au(IMe)(η²-MeCCMe)]⁺.

and enthalpy values instead of Gibbs free energies were presented, consistent with past benchmark studies.

This methodology was used once a benchmarking study with the past results of Belanzoni, Zuccaccia and coworkers[37] was completed (Table S1). In the previous study, the enthalpy – determined by calculations at the B2PLYP/def2-TZVP(COSMO)// BP86/def2-TZVP level of theory – was considered for the nucleophilic attack of [Au(IMe)(η²-MeCCMe)] – i.e. the complex formed from but-2-yne – by triethylene glycol monomethyl ether (gly-OMe) (IMe = 1,3-dimethylimidazol-2-ylidene). This particular alcohol revealed that two alcohol molecules might be helpful to improve both the kinetics and thermodynamics because the internal oxygen atom stabilises the alcohol proton once the oxygen has bonded to the cationic π-gold-alkyne complex **I**; similar conclusions were reported by Ujaque, Lledós and co-workers in their study of gold-catalysed hydrophenoxylation.[61]

From adduct **A**, the barrier (TS) was 10.4 kcal/mol, while **P** was 1.5 kcal/mol higher in energy than **A** (K_{eq} ≈ 0.08 at 298 K) (Figure 1). The use of the implicit solvent model with the optimised gas-phase geometries led to minimal energy differences.

The alcohol was then changed to methanol, yielding similar barrier heights from **A** to **TS** in terms of enthalpy (6.1 kcal/mol) and free energy (15.7 kcal/mol) (Figure 1) *versus* initial reactants **I**. As would be expected, the barrier increases to $\Delta G^{\ddagger}$ = 17.0 kcal/mol from reactants **A**. The Gibbs free energy reveals the relatively low stability of **P**, just 2.5 kcal/mol below the transition state, and 14.5 kcal/mol above **A**. Moreover, the expensive calculations with the def2-TZVP basis set for the geometry optimisations and B2PLYP for the solvent singlet point energy calculations were exchanged for SVP and M06, respectively, with differences in the absolute values of energies of less than 5 kcal/mol. The differences were < 1 kcal/mol using B2PLYP-D3,[69] i.e. including Grimme's dispersion corrections.

This good agreement shows the validity of using Gibbs free energies from M06/TZVP~sdd//BP86/SVP~sdd calculations to study the monogold-catalysed pathway, before more detailed studies of mono and dual gold-catalysed reactions. It is important to note that for the present study Gibbs free energy (G) is considered, instead of enthalpy (H) because of the intermolecular character of the reaction. This will better represent experimental results. Even though dispersion was accounted for in the solvent calculations by means of the use of M06, its quantitative change in the thermal correction was further evaluated, and found to be less than 2 kcal/mol using M06 (see Table S2), and only ca. 1 kcal/mol with D3.[70]

Digold Catalysis

Using the computational scheme used here, M06/TZVP~sdd//BP86/SVP~sdd, Figures S1 and S2 display the free energy profile for the formation of the two monometallic complexes **I** and **II** from [{Au(IPr)}₂(μ-OH)][BF_4] (IPr = 1,3-bis(2,6-diphenylmethyl)imidazol-2-ylidene), and the catalytic cycle, respectively. These species, **I** and **II**, participate in the key carbon-oxygen bond formation step of the hydrophenoxylation reaction, with analogous species being implicated in hydroalkoxylation and hydrocarboxylation reactions. In this previous work, diphenylacetylene was the alkyne substrate and phenol was the nucleophilic alcohol.[65] Here, Figure 2 displays the free energy profile for the reactions of but-2-yne with methanol and diphenylacetylene and phenol, respectively.

All the Density Functional Theory (DFT) preliminary mechanistic studies suggest that the alkoxylation of alkynes proceeds *via* either a direct nucleophilic attack of the η²-alkyne complex **I** ([Au(NHC)(η²-R¹CCR²])⁺ by the alcohol once [Au(NHC)][BF_4] has coordinated the alkyne substrate. Alternatively, this could proceed *via* a dual activation mechanism, where dimer [{Au(NHC)}₂(μ-OH)][BF_4] dissociates, generating alkyne complex **I** plus gold phenoxide complex **II**; the latter is formed when [Au(OH)(NHC)] deprotonates the alcohol substrate. Experimental studies of the hydrophenoxylation reaction had highlighted a negative order in phenol.[65] This was surprising as it clearly has a role to play as a reaction substrate. The reaction of the gold hydroxide fragment with phenol often forms the gold phenoxide **II**,[52] and phenol is a potential proton source during protodeauration, so a positive order in phenol would have been expected. However, the potential for phenol to be involved in several steps on the reaction pathway, as well as in the formation of **I** and **II** from the dimeric precatalyst or in the formation of a digold phenoxide, leads to a complex role for this substrate.

DFT calculations indicate that the binding of [Au(IPr)]⁺ to phenol is energetically favourable (ΔG = -11.1 kcal/mol), although the binding of alkyne is far more so (ΔG = -21.0 kcal/mol). Moreover, the calculations show that there is also the possibility to form a relatively strong hydrogen bond between [Au(OPh)(IPr)] and phenol (ΔG = -1.8 kcal/mol), to be compared with the unfavourable interaction of the same type with water (ΔG = 2.5 kcal/mol).[71] These effects might contribute to the sequestering of the active gold catalyst by phenol, thus changing the ideal 1:1 ratio between **I** and **II** and resulting in the inhibition of the catalytic reaction.

Calculations were carried out on systems bearing a truncated (IMe) and an experimentally-relevant NHC (IPr); the

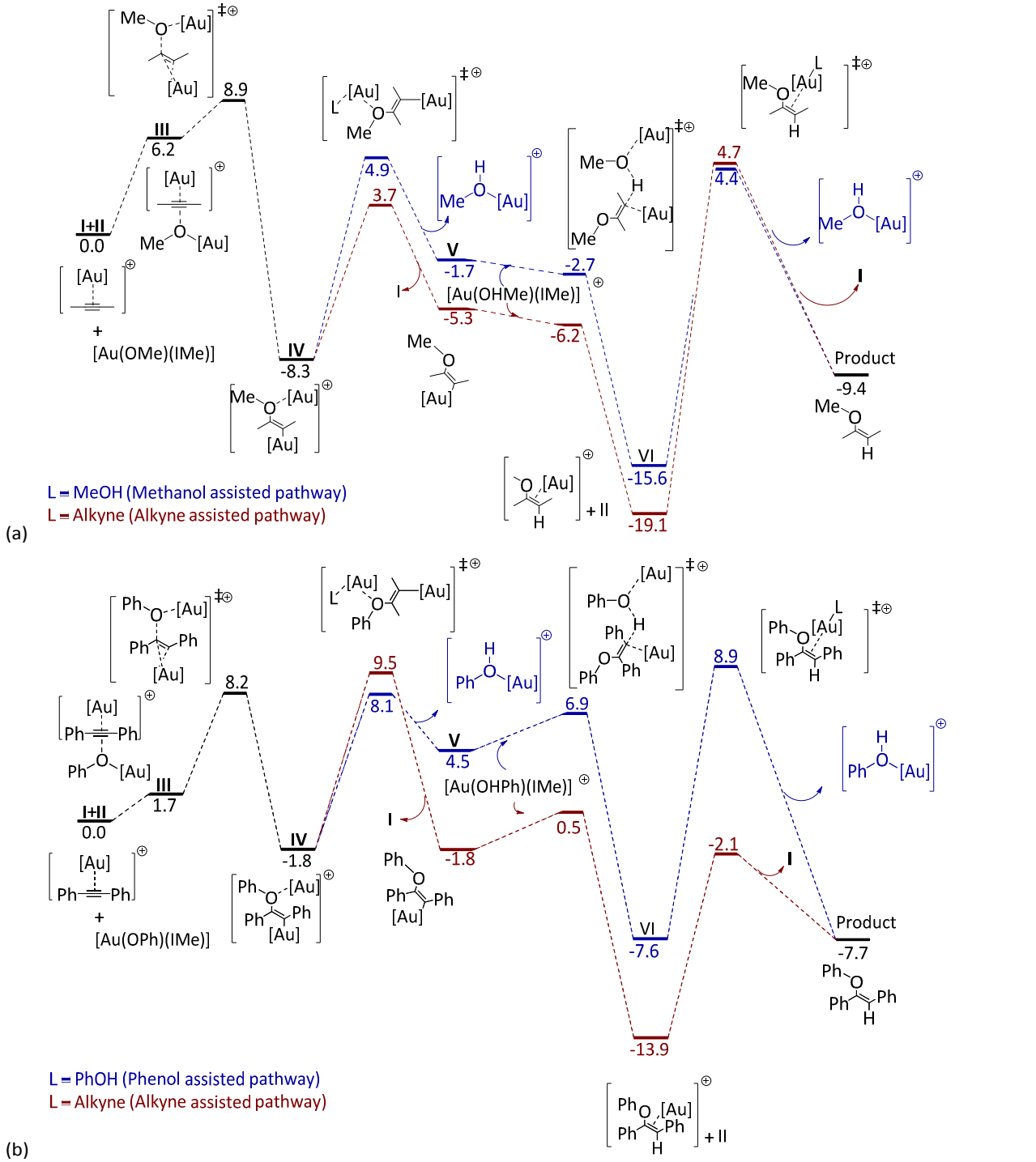

Figure 2. Computed stationary points for the dual-gold catalysed hydroalkoxylation using (a) dimethylacetylene as a substrate and methanol as a nucleophile and (b) (a) diphenylacetylene as a substrate and phenol as a nucleophile (Gibbs energies in chloroform solution are given in kcal/mol relative to complexes **I** and **II**; [Au] = [Au(IMe)].

latter is widely used in gold catalysis and allows comparison with experiments. The pathway with IPr is considered first (Figure S2). The first step is the nucleophilic attack of the alkyne moiety in **I** by the phenoxide group in **II**, forming stable diaurated intermediate **IV** (Figure 2; Figure 3a illustrates **TS(III-IV)**). This proceeds *via* adduct **III** between **I** and **II**, with weak but stabilising interactions between both carbon atoms of alkyne ligand and the oxygen atom in **II**. This adduct **III** is thermodynamically less favourable than diaurated intermediate **IV** (by 5.8 kcal/mol). Kinetically, the alkoxylation requires overcoming a barrier of 15.0 kcal/mol relative to the

separated catalytic species. Intermediate **IV** leads to a σ-monoaurated

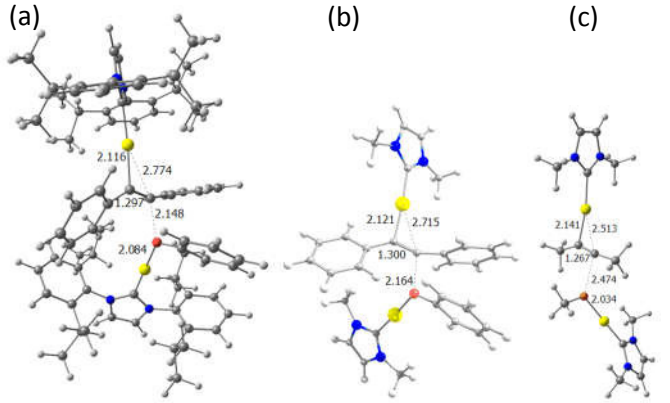

Figure 3. Molecular structures of the computed transition states linking **III** and **IV** corresponding to the diaurated mechanism for (a) NHC = IPr, involving diphenylacetylene and phenol; (b) NHC = IMe, involving diphenylacetylene and phenol, and (c) NHC = IMe, involving but-2-yne and methanol. Distances are in Å.

intermediate **V**; the removal of $[Au(IPr)]^+$ is assisted by a molecule of phenol or alkyne, forming a stable cationic species. As for the relative stability of these competing intermediates, intermediate **V** is 2.1 kcal/mol less stable than **IV**. Kinetically, the alkyne-assisted barrier for the formation of **V** is 2.1 kcal/mol higher in energy relative to the phenol-assisted barrier. However, the resulting cationic species is 8.8 kcal/mol more thermodynamically stable for the alkyne-assisted process (i.e. $[Au(IPr)(\eta^2\text{-MeCCMe})]^+$ versus $[Au(IPr)(OHPh)]^+$.

The next step is the protodeauration of **V** leading to the enol ether intermediate **VI**,[72] which is 11.6 kcal/mol more stable than **V**. The predicted barrier height for this step is only 5.3 kcal/mol; this step is assisted by a cationic gold species bearing phenol. The final step corresponds to the dissociation of $[Au(IPr)]^+$ from the enol ether intermediate **VI** to deliver the *trans*-hydroalkoxylated product,[73] with a free energy change of -13.7 kcal/mol, overcoming a relatively high energy barrier of 15.2 kcal/mol *via* a phenol-assisted pathway, even though this protonation step might be assisted by an acid reagent.[74, 75]

However, it is also possible that this last step is assisted by the alkyne substrate, being just 6.4 kcal/mol higher in energy than the water-assisted pathway,[76] thus releasing the vinyl ether and regenerating complex **I**. Given that **I** and $[Au(IPr)(OHR)]^+$ are close in energy, they will be in equilibrium under the reaction conditions.

In theory, it would be possible for the nucleophilic attack of **I** by **II** to proceed *via* an alternative transition state that would lead ultimately to the (unobserved) cis-alkene product. The barrier for this transition state is 7.2 kcal/mol higher in energy with respect to the barrier that leads to the *trans*-product; the corresponding structures of **IV** differ in energy by 2.7 kcal/mol, with the structure on the *trans*-pathway being lower in energy, as previously reported yet.[56]

Next, the reaction pathway for the simplified catalyst $[Au(IMe)]^+$ - where the 2,6-di(*iso*propyl)phenyl substituents on the NHC are substituted by methyl groups – was calculated (Figure 2). Furthermore, first in Figure 2a the diphenylacetylene was replaced with but-2-yne for the sake of simplicity. Qualitatively the scheme is very similar; however, there are several quantitative energy differences that must be noted. First, because of the reduced steric hindrance of the NHC, the transition state for the nucleophilic attack step is 6.1 kcal/mol lower in energy. However, the subsequent step has a higher barrier because the release of a gold moiety is less favoured because of the reduced steric interaction between the catalyst and substrate. Protodeauration to yield the product is barrierless once the solvent effects are included ($\Delta G‡$ = *ca*. -1 kcal/mol). Finally, the release of the *trans*-product faces a slightly larger barrier than for the reaction with IPr, again due to the reduction in steric interactions. Further, Figure 2b includes the corresponding catalytic pathway with diphenylacetylene and phenol, using the truncated IMe NHC as the ligand for all gold moieties. The relative energy of the transition state in which the C-O bond is formed is close to that shown in Figure 2a, just 0.7 kcal/mol lower, confirming that that for this key step the barrier is mainly affected by the steric hindrance of the substituents on the imidazole ring of the NHC (see Figure 3). The energy barriers for the next steps, the combination of phenol and alkyne substrates displays barriers lower in energy with the alcohol assisting in the removal of the second gold moiety, are approximately 2-3 kcal/mol more favourable for phenol than for methanol. Last but not least, the final transition state is much more favourable with phenol than with methanol, by 5-10 kcal/mol. The C-O bond formation is often thought of as the rate-determining step in experiments, and so there are two important conclusions to deliver from our work: first, this step is mainly due to the sterics of the NHC ligand, and second, the arylic or alkylic nature of the alkyne and alcohol are not significant, bearing a concerted dual gold catalysis.

To understand why the energetic barrier to C-O bond formation decreases when the 2,6-di(*iso*propyl)phenyl substituents are replaced with methyl substituents, steric maps, developed by Cavallo and coworkers, were used to provide insight into the steric environment.[77, 78] By using SambVca (version 2), it is possible to analyse and visualise the first coordination sphere around the metal where the catalysis takes place.[79-81] The quadrants around gold in the IMe and IPr complexes were plotted as steric contour maps (Figure 4). It is evident from Figure 4 that for these two Au complexes, species bearing IPr present significantly more steric bulk. The percent buried volume ($\%V_{bur}$) for complex **I** bearing IPr is much larger (39%) than for the simplified IMe complex (26%). Considering individual quadrants, the difference is stark, with values of 43/35/43/35% for IPr and 26/25/26/25% for IMe. The more sterically hindered environment around the IPr complex might be expected to make the nucleophilic attack of either an external alcohol or the phenoxide complex **II** more difficult. The huge differences in absolute value confirm that both types of NHCs are extremely different, and the data for IMe must be tackled cautiously since the system is incredibly less sterically hindered. For the C-O bond formation, which is the rate determining step in the real system, this barrier is extremely sensitive to the nature of the steric hindrance due to the NHC ligand.

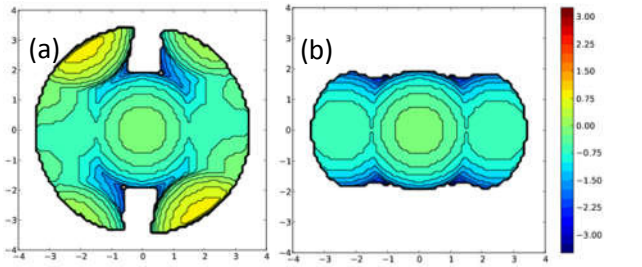

Figure 4. Topographical steric maps of the NHC ligands in $[Au(NHC)(\eta^2\text{-MeCCMe})]^+$ for (a) IPr and (b) IMe NHCs studied herein. The Au atom is at the origin and the Au-C_{NHC} bond is aligned with the z-axis. The isocontour curves of the steric maps are given in Å.

To summarise the results of the dual gold catalysed mechanism, the overall process is thermodynamically favourable, even once the entropic penalty of this bimolecular reaction is included. More importantly, considering acetylene and phenol, the key barrier – corresponding to the attack of **I** by **II**, leading to **IV** – is 15.0 or 8.2 kcal/mol for the IPr or IMe systems, respectively.

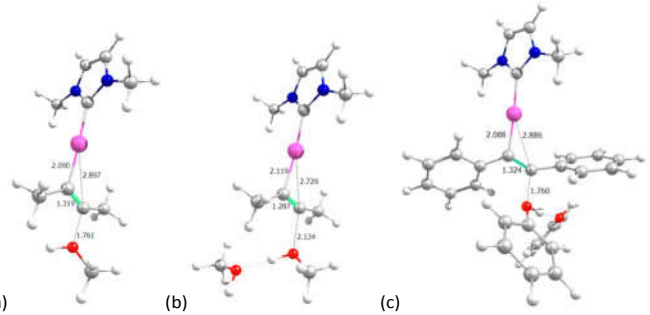

Figure 5. Molecular structures of the computed transition states corresponding to the monoaurated mechanism for the *in silico* NHC = IMe system, involving: but-2-yne and (a) one or (b) molecules of methanol, or two molecules of phenol and (c) diphenylacetylene.

Calculations on the monogold-catalysed reaction of but-2-yne using the simplified NHC ligand (IMe) reveal that the nucleophilic attack of the alcohol on complex **I** is not trivial (See Table 1), both in kinetic and thermodynamic terms. With methanol as the alcohol the barrier is 26.9 or 22.9 kcal/mol, depending on whether one or two molecules of methanol are involved. With diphenylacetylene and phenol only the two alcohol transition state is located, and is found to display a high energy barrier of 34.4 kcal/mol. Considering the differences between aryl and alkyl substituents on both the alkyne and the alcohol, the alkyl character of the alkyne is found to be unimportant, while the nature of the alcohol becomes crucial, since with but-2-yne and phenol the barrier is 34.8 kcal/mol, whereas for diphenylacetylene and methanol the barrier decreases to 25.8 kcal/mol. Figure 5 illustrates the transition state for the C-O bond formation for the truncated IMe systems, and further structural and electronic characterization of the monogold mechanism is included in the Supporting Information, including the 1,1,1,3,3,3-hexafluorobut-2-yne substrate as well.

The second molecule of alcohol can stabilise the developing cationic charge on the alcoholic proton when forming the C-O bond; this is achieved by forming a hydrogen bond in the transition state. The next intermediate is nearly isoenergetic with respect to the preceding transition state, but it must be noted that this intermediate might be partially stabilized by interactions with the counterion of the metal catalyst (e.g. BF_4).[82, 83] The predicted barriers are consistent with the reaction temperatures that are required to achieve these reactions experimentally in satisfactory yield within reasonable reaction times. However, with more complex and useful substrates (such as those with aryl-substituted substrates) the barriers become prohibitive, not only due to the steric properties, but also the electronic properties of the substrate.

With the mono- and digold-catalysed mechanisms described by DFT calculations, and even though the digold mechanism is found to be strongly favored with respect to the monogold one when the catalyst concentration is relatively not low, the role of each species involved was probed.

The results from the monogold catalysed pathway can be compared to those from the dual gold-catalysed mechanism. In the latter, the highest energy barrier is 15.0 kcal/mol for the hydrophenoxylation of diphenylacetylene to be compared with 8.2 kcal/mol bearing the IMe NHC ligand. The latter value can be compared to 34.4 kcal/mol for the monogold-catalysed pathway, where two phenol molecules participate. Thus, this C-O bond formation for the monoaurated process is 26.2 kcal/mol more expensive.

Table 1. Nucleophilic attack of the π-gold-alkyne species **I** by the alcohol. Gibbs energies in chloroform solution are given in kcal/mol, **A** = adduct; **TS** = transition state; **P** = product).

	Alkyne	Alcohol	E	H	G
I		-	0.0	0.0	0.0
A			-1.7	-0.3	8.0
TS		1 MeOH	13.4	14.4	26.9
P			13.6	15.3	27.7
A			-7.6	-4.7	12.0
TS		2 MeOH	0.0	2.4	22.9
P			-2.9	0.0	23.1
A			-1.8	-0.7	6.5
TS		1 PhOH	-	-	-
P			-	-	-
A			-8.3	-5.6	11.1
TS		2 PhOH	10.5	12.2	34.8
P			8.9	11.0	34.6
	Alkyne	**Alcohol**	**E**	**H**	**G**
I		-	0.0	0.0	0.0
A			-3.2	-1.7	7.4
TS		1 MeOH	13.0	15.0	29.4
P			-4.1	-3.0	11.9
A			-9.5	-6.4	10.7
TS		2 MeOH	-0.4	4.1	25.8
P			-8.5	-6.8	18.9
A			-2.2	-0.9	7.5
TS		1 PhOH	-	-	-
P			-	-	-
A			-9.8	-7.0	12.0
TS		2 PhOH	8.0	9.6	34.4
P			3.6	4.5	31.2

The analysis of the geometry of the transition state (**TS**) turns out to be fundamental, describing early or late transition states. When the C···O distance is close to 1.5 Å which is similar to the C-O bond distance in **P**, the corresponding **TS** can be considered a late transition state. Furthermore, when the alkyne has aryl substituents, the **TS** structures have slightly less late character. On the other hand, when two alcohol molecules are involved, the second alcohol molecule somewhat stabilises the developing positive charge on the alcohol proton, thus dramatically reducing the later transition state character.

The character of the carbon-carbon bond in η^2-alkyne complex **I** is essentially unaffected once the alcohol bonds to either of the carbon atoms, with a small elongation (< 0.09 Å) in all structures studied. In the corresponding step of the dual gold-catalysed mechanism (see **TS(III-IV)** in Figure 3), the C···O distance in the transition state is 2.474 Å (versus 2.134 Å for the monogold pathway), confirming that the transition state has less late character in the dual gold-catalysed mechanism.

For a more detailed analysis of the structural changes during the hydroalkoxylation, Mayer Bond Orders (MBO) of the main distances involved in the C-O bond formation are collected in Table S2. The MBO for the former C-C of the alkyne does not change whereas the Au-C MBOs change dramatically. However, the MBOs for the Au-C bonds span a range from 0.6 to 0.7, and are thus rather far from 1.0 in the initial η^2-alkyne complex **I**. As would be expected, one Au-C bond sees an increase in MBO of around 0.2 – forming a formal Au-C σ-bond in **P** – while the MBO of the other Au-C bond decreases to 0.1 or lower in **P**. For the dual gold-catalysed mechanism, in the nucleophilic attack (**III** to **IV**) the MBO of the C-C bond decreases from 2.008 to 1.837. Thus, a significant difference of 0.171 is observed, to be compared with the meaningless values of 0.006 for two phenol units, in the monogold-catalysed pathway. The decrease is sharper with but-2-yne and the nucleophile methanol, by 0.080 and 0.147 for one or two methanol molecules, respectively. Furthermore, the new C-O bond in **IV** displays a MBO of 0.772, significantly higher than 0.786 in the monogold-catalysed pathway (with two phenol molecules, respectively).

Conclusions

Gold complexes are amongst the most efficient catalysts for the hydroalkoxylation of alkynes. Herein we have carried out a detailed comparison of mono- and dual gold-catalysed mechanisms, prompted by recent studies of the nucleophilic attack recently Zuccaccia and coworkers with a simplified Au based catalyst, and recent collaborations with the Nolan group to examine dual gold-catalysed processes. If both gold moieties are accessible, DFT calculations have revealed that the dual gold-catalysed mechanism is more facile because the formation of phenoxide **II** activates the alcohol for nucleophilic attack; this leads to a dramatic (>> 10 kcal/mol) decrease in the barrier for nucleophilic attack. In contrast, less acidic alcohols do not require this activation and are capable of undergoing reaction *via* mono-gold catalysis.

It is important to mention that in this study we have not taken into consideration the role of the counter anion, although it has been postulated that the counter anion may participate in the monometallic mechanism. However, this agent would basically stabilise the alcohol proton as the C-O bond is formed and positive charge accumulates at oxygen, which is a role that can also be fulfilled by a second alcohol molecule. We would expect that the kinetics of the reaction would not be affected dramatically, but that the thermodynamics might.

The reaction of η^2-complex **I** with alcohols is difficult from kinetic and thermodynamic points of view, with barriers above 20 kcal/mol, while the dual gold-catalysed mechanism has no barrier higher than 10 kcal/mol (for the simple case of methanol and but-2-yne). Moreover, the simplification of the *N*-heterocyclic carbene (NHC) ligand in the calculations – i.e. the replacement of 2,6-di*iso*propylphenyl with methyl – decreases the energy barrier. When the Au-IPr catalyst is considered, the barrier for the alkoxylation with the same substrates requires a barrier of more than 30 kcal/mol to be overcome, which is likely to be unfeasible without elevated temperatures.

Conceptual DFT, using the concepts of chemical hardness and electrophilicity, allow the rationalisation of the potential catalytic performance using different kind of alkyne substrates and alcohols. These results show that the reaction is favoured for alkyne substrates with electron-withdrawing substituents such as trifluoromethyl groups, and in the presence of alkyl alcohols like methanol or ethanol instead of aromatic solvents such as phenol.

These results demonstrate that the monogold mechanism is nearly impossible, except when the nucleophilic attack of complex **I** is favored kinetically and thermodynamically by a counteranion or by a co-catalyst in the dual metal system, as very recently Cazin and coworkers have demonstrated experimentaly by a heterobimetallic Cu-NHC/Au-NHC system.[84]. In this particular study, this co-catalyst is a gold(I) phenoxide (**II**). Only with synergetic cooperation between the two gold units the C-O bond formation, i.e. the rate determining step, the process turns out to be more feasible. However, studies that focus on monometallic catalysis allow for better understanding of the role of the substituents on the alkyne and alcohol. From the results presented here, electron withdrawing groups on the alkyne moiety and an alkyl alcohol instead of an aryl alcohol both decrease the barrier to alkoxylation. Therefore, this study contributes to a better understanding about the interactions involved in the transformation of alkynes to functionalised *trans*-alkenes. Moreover, these DFT calculations also confirm that the barrier of the transition state that leads to the *cis*-species is significantly higher in energy. In conclusion, this study provides useful information that will enable future *in silico* studies of mechanism and structure/activity relationships. By DFT calculations it is shown that the dual gold mechanism is favoured, but this does not exclude the monogold catalyst, as stated recently,[47] especially if the catalyst loading is low. It will depend on the facility to join two metal moieties. However, it is demonstrated that the presence of a second gold moiety leads preferentially to the reaction proceeding through the digold mechanism.

Computational Details

All the static DFT calculations were performed at the GGA level with the Gaussian 09 set of programs[85] by using the BP86 functional of Becke and Perdew.[86-88] The electronic configurations of the molecular systems were described with the standard split-valence basis set by using the polarization function of Ahlrichs and coworkers for hydrogen, carbon, nitrogen and oxygen (SVP keyword in Gaussian 09).[89] For gold, the quasi-relativistic Stuttgart/Dresden effective core potential with the associated valence basis set (standard SDD keywords in Gaussian 09) was used.[90, 91] The geometry optimisations were carried out without symmetry constraints, and the stationary points were characterised by analytical frequency calculations. Single-point calculations of the BP86-optimised geometries were performed using the M06 functional[92] that includes dispersion with the triple-zeta basis set of Weigend and Ahlrichs for main-group atoms (TZVP keyword in Gaussian),[93] whereas for gold the SDD basis set was employed. The polarisable continuous model (PCM) was also used in these single-point calculations to model the solvent effects, using chloroform as the solvent.[94, 95] The reported free energies in this work include energies obtained at the M06/TZVP level of theory corrected with zero-point energies, thermal corrections and entropy effects evaluated at 298 K and 1 atm (values at 1354 atm can be found Table S1)[96-98] with the BP86/SVP method in the gas phase.

Acknowledgements

A.P. thanks the Spanish MINECO for a project CTQ2014-59832-JIN. E.C. and A.P. thank Xarxa de Química Teòrica i Computacional for a VALCHEM2016 project. D.J.N. thanks the University of Strathclyde for a Chancellor's Fellowship and support from the Global Engagements Fund and the WestCHEM Early Career Researcher Exchanges Fund. O.F.G.B. thanks Universidad de Guanajuato for funding the Master Thesis. We thank the referees for helpful comments and suggestions.

Notes and references

1. D. J. Gorin and F. D. Toste, *Nature*, 2007, **446**, 395-403.
2. A. S. K. Hashmi, *Nature*, 2007, **449**, 292-293.
3. S. P. Nolan, *Nature*, 2007, **445**, 496-497.
4. M. Rudolph and A. S. K. Hashmi, *Chem. Soc. Rev.*, 2012, **41**, 2448-2462.
5. E. Jiménez-Núñez and A. M. Echavarren, *Chem. Rev.*, 2008, **108**, 3326-3350.
6. G. Abbiati and E. Rossi, *Beilstein J. Org. Chem.*, 2014, **10**, 481-513.
7. H. A. Wegner and M. Auzias, *Angew. Chem. Int. Ed.*, 2011, **50**, 8236-8247.
8. M. Bandini, *Chem. Soc. Rev.*, 2011, **40**, 1358-1367.
9. D. Pflasterer and A. S. K. Hashmi, *Chem. Soc. Rev.*, 2016, **45**, 1331-1367.
10. A. S. K. Hashmi, *Chem. Rev.*, 2007, **107**, 3180-3211.
11. P. H.-Y. Cheong, P. Morganelli, M. R. Luzung, K. N. Houk and F. D. Toste, *J. Am. Chem. Soc.*, 2008, **130**, 4517-4526.
12. Y. Odabachian, X. F. Le Goff and F. Gagosz, *Chem. Eur. J.*, 2009, **15**, 8966-8970.
13. S. Sun, J. Kroll, Y. Luo and L. Zhang, *Synlett*, 2012, **2012**, 54-56.
14. L. Ye, Y. Wang, D. H. Aue and L. Zhang, *J. Am. Chem. Soc.*, 2012, **134**, 31-34.
15. A. Gómez-Suárez, Y. Oonishi, S. Meiries and S. P. Nolan, *Organometallics*, 2013, **32**, 1106-1111.
16. Y. Oonishi, A. Gómez-Suárez, A. R. Martin and S. P. Nolan, *Angew. Chem. Int. Ed.*, 2013, **52**, 9767-9771.
17. R. M. P. Veenboer, S. Dupuy and S. P. Nolan, *ACS Catal.*, 2015, **5**, 1330-1334.
18. S. Dupuy, D. Gasperini and S. P. Nolan, *ACS Catal.*, 2015, **5**, 6918-6921.
19. I. Braun, A. M. Asiri and A. S. K. Hashmi, *ACS Catal.*, 2013, **3**, 1902-1907.
20. A. Gómez-Suárez and S. P. Nolan, *Angew. Chem. Int. Ed.*, 2012, **51**, 8156-8159.
21. A. S. K. Hashmi, *Acc. Chem. Res.*, 2014, **47**, 864-876.
22. A. S. K. Hashmi, T. Lauterbach, P. Nösel, M. H. Vilhelmsen, M. Rudolph and F. Rominger, *Chem. Eur. J.*, 2013, **19**, 1058-1065.
23. A. S. K. Hashmi, I. Braun, P. Nösel, J. Schädlich, M. Wieteck, M. Rudolph and F. Rominger, *Angew. Chem. Int. Ed.*, 2012, **51**, 4456-4460.
24. M. H. Larsen, K. N. Houk and A. S. K. Hashmi, *J. Am. Chem. Soc.*, 2015, **137**, 10668-10676.
25. W. Wang, G. B. Hammond and B. Xu, *J. Am. Chem. Soc.*, 2012, **134**, 5697-5705.
26. C. Nieto-Oberhuber, S. López and A. M. Echavarren, *J. Am. Chem. Soc.*, 2005, **127**, 6178-6179.
27. H. Clavier and S. P. Nolan, *Chem. Commun.*, 2010, **46**, 841-861.
28. M. Alcarazo, T. Stork, A. Anoop, W. Thiel and A. Fürstner, *Angew. Chem. Int. Ed.*, 2010, **49**, 2542-2546.
29. S. Díez-González, N. Marion and S. P. Nolan, *Chem. Rev.*, 2009, **109**, 3612-3676.
30. S. V. C. Vummaleti, D. J. Nelson, A. Poater, A. Gomez-Suarez, D. B. Cordes, A. M. Z. Slawin, S. P. Nolan and L. Cavallo, *Chem. Sci.*, 2015, **6**, 1895-1904.
31. D. J. Nelson and S. P. Nolan, *Chem. Soc. Rev.*, 2013, **42**, 6723-6753.
32. D. Marchione, L. Belpassi, G. Bistoni, A. Macchioni, F. Tarantelli and D. Zuccaccia, *Organometallics*, 2014, **33**, 4200-4208.
33. S. P. Nolan, *Acc. Chem. Res.*, 2011, **44**, 91-100.
34. M. C. Blanco Jaimes, C. R. N. Böhling, J. M. Serrano-Becerra and A. S. K. Hashmi, *Angew. Chem. Int. Ed.*, 2013, **52**, 7963-7966.
35. M. C. Blanco Jaimes, F. Rominger, M. M. Pereira, R. M. B. Carrilho, S. A. C. Carabineiro and A. S. K. Hashmi, *Chem. Commun.*, 2014, **50**, 4937-4940.
36. R. E. M. Brooner and R. A. Widenhoefer, *Angew. Chem. Int. Ed.*, 2013, **52**, 11714-11724.
37. M. Trinchillo, P. Belanzoni, L. Belpassi, L. Biasiolo, V. Busico, A. D'Amora, L. D'Amore, A. Del Zotto, F. Tarantelli, A. Tuzi and D. Zuccaccia, *Organometallics*, 2016, **35**, 641-654.
38. G. Ciancaleoni, L. Biasiolo, G. Bistoni, A. Macchioni, F. Tarantelli, D. Zuccaccia and L. Belpassi, *Organometallics*, 2013, **32**, 4444-4447.
39. D. Zuccaccia, L. Belpassi, F. Tarantelli and A. Macchioni, *J. Am. Chem. Soc.*, 2009, **131**, 3170-3171.

40. D. Zuccaccia, L. Belpassi, L. Rocchigiani, F. Tarantelli and A. Macchioni, *Inorg. Chem.*, 2010, **49**, 3080-3082.
41. G. Ciancaleoni, L. Belpassi, D. Zuccaccia, F. Tarantelli and P. Belanzoni, *ACS Catal.*, 2015, **5**, 803-814.
42. L. Biasiolo, A. Del Zotto and D. Zuccaccia, *Organometallics*, 2015, **34**, 1759-1765.
43. L. Rocchigiani, M. Jia, M. Bandini and A. Macchioni, *ACS Catal.*, 2015, **5**, 3911-3915.
44. A. Zhdanko and M. E. Maier, *ACS Catal.*, 2014, **4**, 2770-2775.
45. L. Biasiolo, M. Trinchillo, P. Belanzoni, L. Belpassi, V. Busico, G. Ciancaleoni, A. D'Amora, A. Macchioni, F. Tarantelli and D. Zuccaccia, *Chem. Eur. J.*, 2014, **20**, 14594-14598.
46. J. Roithová, Š. Janková, L. Jašíková, J. Váňa and S. Hybelbauerová, *Angew. Chem. Int. Ed.*, 2012, **51**, 8378-8382.
47. L. Jašíková, M. Anania, S. Hybelbauerová and J. Roithová, *J. Am. Chem. Soc.*, 2015, **137**, 13647-13657.
48. V. D'Elia, H. Dong, A. J. Rossini, C. M. Widdifield, S. V. C. Vummaleti, Y. Minenkov, A. Poater, E. Abou-Hamad, J. D. A. Pelletier, L. Cavallo, L. Emsley and J.-M. Basset, *J. Am. Chem. Soc.*, 2015, **137**, 7728-7739.
49. V. D'Elia, A. A. Ghani, A. Monassier, J. Sofack-Kreutzer, J. D. A. Pelletier, M. Drees, S. V. C. Vummaleti, A. Poater, L. Cavallo, M. Cokoja, J.-M. Basset and F. E. Kühn, *Chem. Eur. J.*, 2014, **20**, 11870-11882.
50. R. S. Ramón, S. Gaillard, A. Poater, L. Cavallo, A. M. Z. Slawin and S. P. Nolan, *Chem. Eur. J.*, 2011, **17**, 1238-1246.
51. S. Gaillard, A. M. Z. Slawin and S. P. Nolan, *Chem. Commun.*, 2010, **46**, 2742-2744.
52. N. Ibrahim, M. H. Vilhelmsen, M. Pernpointner, F. Rominger and A. S. K. Hashmi, *Organometallics*, 2013, **32**, 2576-2583.
53. J. D. Egbert, A. M. Z. Slawin and S. P. Nolan, *Organometallics*, 2013, **32**, 2271-2274.
54. A. C. H. Jans, A. Gómez-Suárez, S. P. Nolan and J. N. H. Reek, *Chem. Eur. J.*, 2016, **22**, 14836-14839.
55. M. R. Kuram, M. Bhanuchandra and A. K. Sahoo, *J. Org. Chem.*, 2010, **75**, 2247-2258.
56. M. E. Richard, D. V. Fraccica, K. J. Garcia, E. J. Miller, R. M. Ciccarelli, E. C. Holahan, V. L. Resh, A. Shah, P. M. Findeis and R. A. S. Jr, *Beilstein J. Org. Chem.*, 2013, **9**, 2002-2008.
57. G. Ciancaleoni, S. Rampino, D. Zuccaccia, F. Tarantelli, P. Belanzoni and L. Belpassi, *J. Chem. Theor. Comput.*, 2014, **10**, 1021-1034.
58. A. Zhdanko and M. E. Maier, *Chem. Eur. J.*, 2014, **20**, 1918-1930.
59. Z. J. Wang, D. Benitez, E. Tkatchouk, W. A. Goddard Iii and F. D. Toste, *J. Am. Chem. Soc.*, 2010, **132**, 13064-13071.
60. A. Zhdanko and M. E. Maier, *Angew. Chem. Int. Ed.*, 2014, **53**, 7760-7764.
61. G. Kovács, A. Lledós and G. Ujaque, *Organometallics*, 2010, **29**, 3252-3260.
62. C. A. Urbina-Blanco, A. Poater, T. Lebl, S. Manzini, A. M. Z. Slawin, L. Cavallo and S. P. Nolan, *J. Am. Chem. Soc.*, 2013, **135**, 7073-7079.
63. M. García-Melchor, M. C. Pacheco, C. Nájera, A. Lledós and G. Ujaque, *ACS Catal.*, 2012, **2**, 135-144.
64. S. Manzini, A. Poater, D. J. Nelson, L. Cavallo and S. P. Nolan, *Chem. Sci.*, 2014, **5**, 180-188.
65. A. Gómez-Suárez, Y. Oonishi, A. R. Martin, S. V. C. Vummaleti, D. J. Nelson, D. B. Cordes, A. M. Z. Slawin, L. Cavallo, S. P. Nolan and A. Poater, *Chem. Eur. J.*, 2016, **22**, 1125-1132.
66. S. Grimme, *J. Chem. Phys.*, 2006, **124**, 034108.
67. R. Kang, H. Chen, S. Shaik and J. Yao, *J. Chem. Theor. Comput.*, 2011, **7**, 4002-4011.
68. R. Kang, W. Lai, J. Yao, S. Shaik and H. Chen, *J. Chem. Theor. Comput.*, 2012, **8**, 3119-3127.
69. L. Goerigk and S. Grimme, *J. Chem. Theor. Comput.*, 2011, **7**, 291-309.
70. S. Grimme, S. Ehrlich and L. Goerigk, *J. Comput. Chem.*, 2011, **32**, 1456-1465.
71. S. E. Kegley, C. J. Schaverien, J. H. Freudenberger, R. G. Bergman, S. P. Nolan and C. D. Hoff, *J. Am. Chem. Soc.*, 1987, **109**, 6563-6565.
72. Y. Zhu, C. S. Day and A. C. Jones, *Organometallics*, 2012, **31**, 7332-7335.
73. R. S. Paton and F. Maseras, *Org. Lett.*, 2009, **11**, 2237-2240.
74. A. Hossein Bagi, Y. Khaledi, H. Ghari, S. Arndt, A. S. K. Hashmi, B. F. Yates and A. Ariafard, *J. Am. Chem. Soc.*, 2016, **138**, 14599-14608.
75. J. Schießl, M. Rudolph and A. S. K. Hashmi, *Adv. Synth. Catal.*, 2017, **359**, 639-653.
76. C. M. Krauter, A. S. K. Hashmi and M. Pernpointner, *ChemCatChem*, 2010, **2**, 1226-1230.
77. L. Falivene, R. Credendino, A. Poater, A. Petta, L. Serra, R. Oliva, V. Scarano and L. Cavallo, *Organometallics*, 2016, **35**, 2286-2293.
78. A. Poater, B. Cosenza, A. Correa, S. Giudice, F. Ragone, V. Scarano and L. Cavallo, *Eur. J. Inorg. Chem.*, 2009, **2009**, 1759-1766.
79. L. Cavallo, A. Correa, C. Costabile and H. Jacobsen, *J. Organomet. Chem.*, 2005, **690**, 5407-5413.
80. A. Poater, F. Ragone, S. Giudice, C. Costabile, R. Dorta, S. P. Nolan and L. Cavallo, *Organometallics*, 2008, **27**, 2679-2681.
81. A. Gomez-Suarez, D. J. Nelson and S. P. Nolan, *Chem Commun (Camb)*, 2017, **53**, 2650-2660.
82. M. Gatto, P. Belanzoni, L. Belpassi, L. Biasiolo, A. Del Zotto, F. Tarantelli and D. Zuccaccia, *ACS Catal.*, 2016, **6**, 7363-7376.
83. L. D'Amore, G. Ciancaleoni, L. Belpassi, F. Tarantelli, D. Zuccaccia and P. Belanzoni, *Organometallics*, 2017, DOI: 10.1021/acs.organomet.7b00377.
84. F. Lazreg, S. Guidone, A. Gomez-Herrera, F. Nahra and C. S. J. Cazin, *Dalton Trans.*, 2017, **46**, 2439-2444.
85. M. J. Frisch, G. W. Trucks, H. B. Schlegel, G. E. Scuseria, M. A. Robb, J. R. Cheeseman, G. Scalmani, V. Barone, G. A. Petersson, H. Nakatsuji, X. Li, M. Caricato, A. V. Marenich, J. Bloino, B. G. Janesko, R. Gomperts, B. Mennucci, H. P. Hratchian, J. V. Ortiz, A. F. Izmaylov, L. Sonnenberg, D. Williams-Young, F. Ding, F. Lipparini, F. Egidi, J. Goings, B. Peng, A. Petrone, T. Henderson, D. Ranasinghe, J. Zakrzewski, J. Gao, N. Rega, G. Zheng, W. Liang, M. Hada, M. Ehara, K. Toyota, R. Fukuda, J. Hasegawa, M. Ishida, T. Nakajima, Y. Honda, O. Kitao, H. Nakai, T. Vreven, K. Throssell, J. Montgomery, J. A., J. E. Peralta, F. Ogliaro, M. J. Bearpark, J. J. Heyd, E. N. Brothers, K. N. Kudin, V. N. Staroverov, T. A. Keith, R. Kobayashi, J. Normand, K. Raghavachari, A. P. Rendell, J. C. Burant, S. S. Iyengar, J. Tomasi, M. Cossi, J. M. Millam, M. Klene, C. Adamo, R. Cammi, J. W. Ochterski, R. L. Martin, K. Morokuma, O. Farkas, J. B. Foresman and D. J. Fox, *Journal*, 2009.

86. A. D. Becke, *Phys. Rev. A.: Mol., Opt. Phys.*, 1988, **38**, 3098-3100.
87. J. P. Perdew, *Phys. Rev. B.: Condens. Mater.*, 1986, **33**, 8822-8824.
88. J. P. Perdew, *Phys. Rev. B.: Condens. Mater.*, 1986, **34**, 7406-7406.
89. A. Schäfer, H. Horn and R. Ahlrichs, *J. Chem. Phys.*, 1992, **97**, 2571-2577.
90. W. Küchle, M. Dolg, H. Stoll and H. Preuss, *J. Chem. Phys.*, 1994, **100**, 7535-7542.
91. T. Leininger, A. Nicklass, H. Stoll, M. Dolg and P. Schwerdtfeger, *J. Chem. Phys.*, 1996, **105**, 1052-1059.
92. Y. Zhao and D. G. Truhlar, *Theor. Chem. Acc.*, 2008, **120**, 215-241.
93. F. Weigend and R. Ahlrichs, *Physical Chemistry Chemical Physics*, 2005, **7**, 3297-3305.
94. V. Barone and M. Cossi, *J. Phys. Chem. A*, 1998, **102**, 1995-2001.
95. J. Tomasi and M. Persico, *Chem. Rev.*, 1994, **94**, 2027-2094.
96. R. L. Martin, P. J. Hay and L. R. Pratt, *J. Phys. Chem. A*, 1998, **102**, 3565-3573.
97. S. Manzini, A. Poater, D. J. Nelson, L. Cavallo, A. M. Z. Slawin and S. P. Nolan, *Angew. Chem. Int. Ed.*, 2014, **53**, 8995-8999.
98. A. Poater, E. Pump, S. V. C. Vummaleti and L. Cavallo, *J. Chem. Theor. Comput.*, 2014, **10**, 4442-4448.

